The Prefrontal Cortex Modulates Category Selectivity in Human Extrastriate Cortex

Brian T. Miller, Jason Vytlacil, David Fegen, Suraj Pradhan, and Mark D'Esposito

Abstract

■ Different categories of visual objects evoke distinct stimulus-evoked sensory responses in extrastriate visual cortex. Although numerous lines of evidence support a distinct representational neural architecture, the mechanisms underlying the modulation of the category selectivity by top–down influences remains uncertain. In this study, we investigate the causal role of the PFC in the modulation of evoked activity to face and scene stimuli in the extrastriate cortex. We used two experimental approaches to disrupt prefrontal cortical function—repetitive TMS to PFC in healthy participants (Experiment 1) and focal PFC lesions in stroke patients (Experiment 2). After these perturbations to normal PFC function (pre- vs. post-TMS and lesion vs. intact hemisphere), stimulus-evoked activity in extrastriate cortex exhibited less distinct category selectivity to faces and scenes. These two experiments provide convergent evidence highlighting a direct role of PFC in the top–down modulation of bottom–up visual signals. ■

INTRODUCTION

Different categories of visual objects evoke distinct patterns of bottom–up sensory activity in extrastriate visual cortex. Distinct representational architecture in the ventral visual stream allows the brain to rapidly parse bottom–up visual signals into discrete object categories—thus forming the foundation of our ability to flexibly and accurately interact with our visual world. Previous evidence suggests that several aspects of bottom–up visual processing—including the gain (Chawla, Rees, & Friston, 1999; Luck, Chelazzi, Hillyard, & Desimone, 1997), tuning (Serences, Saproo, Scolari, Ho, & Muftuler, 2009; Murray & Wojciulik, 2004; Haenny & Schiller, 1988), synchronization (Womelsdorf et al., 2007), and temporal properties (Gazzaley et al., 2008) of evoked sensory signals—may be sculpted by top–down signals that modify incoming sensory signals in a goal- and context-driven manner. Many of these top–down signals are hypothesized to originate from multimodal subregions in the PFC (Miller & D'Esposito, 2005; Miller & Cohen, 2001). The preliminary study reported here attempted to obtain causal evidence for a role of PFC-mediated top–down signals in the tuning of category selectivity in extrastriate cortex.

The PFC emerges as a candidate source of these signals given the extensive and reciprocal anatomical connectivity between subregions of PFC and multiple levels of the visual system (Webster, Bachevalier, & Ungerleider, 1994). Further, a wealth of indirect evidence from electrophysiology (e.g., Rainer, Asaad, & Miller, 1998) and neuroimaging (e.g., Druzgal & D'Esposito, 2003) studies have highlighted PFC as an area consistently engaged when sensory processing must be biased in a goal-directed manner. This evidence, however, is limited given that measurement of the engagement of PFC with these physiological techniques cannot specify a direction of influence. Studies of the effect of PFC lesions on activity within posterior visual cortex would provide evidence for the direction of interactions not only across distributed brain systems but also in a causal fashion (Miller & D'Esposito, 2005). The ability to tease apart physiological changes in sensory cortices that are driven by bottom–up versus top–down influences remains a prominent methodological challenge for cognitive neuroscience investigations in both animal and human models. One of the few published studies providing causal evidence of top–down influences showed that deactivation of PFC via cryogenic depression in monkeys (Fuster, Bauer, & Jervey, 1985) not only attenuated inferotemporal cortex maintenance signals during the delay period of a working memory task but also caused a marked decrease in stimulus selectivity of these temporal cortex neurons. Importantly, this loss of selectivity was not just present during the maintenance period but also during the bottom–up sensory response to the cue—during which a cell's preference for a given stimulus class (in the case of this experiment, color) often disappeared after frontal cooling. By using a novel combination of methodologies, this experiment provided invaluable insight that PFC influences mnemonic and sensory signals in extrastriate cortex in a top–down manner.

Investigations of disrupted PFC function with concurrent physiological measures of posterior cortical activity

University of California, Berkeley

remain scarce (see Barcelo, Suwazono, & Knight, 2000; Yamaguchi & Knight, 1990). As a result, most theories regarding how PFC biases response properties of posterior cortex and whether PFC is critical for this modulation remain speculative.

Different object categories are represented by spatially distributed yet overlapping assemblies in extrastriate visual cortex (Op de Beeck, Haushofer, & Kanwisher, 2008; Haxby et al., 2001). To investigate whether PFC causally influences the selectivity of category representations within extrastriate cortex, we performed two experiments to explore the impact of PFC disruption on the patterns of activity evoked during the performance of a simple perceptual task using face and scene stimuli with minimal mnemonic demands. In Experiment 1, we examined the selectivity of visual responses to faces and scene stimuli in healthy control participants after transient PFC disruption with TMS. In Experiment 2, we examined category selectivity in patients with focal PFC damage due to stroke. The findings in both experiments provide convergent evidence showing that PFC disruption can lead to less distinctive representations of object categories in the extrastriate cortex.

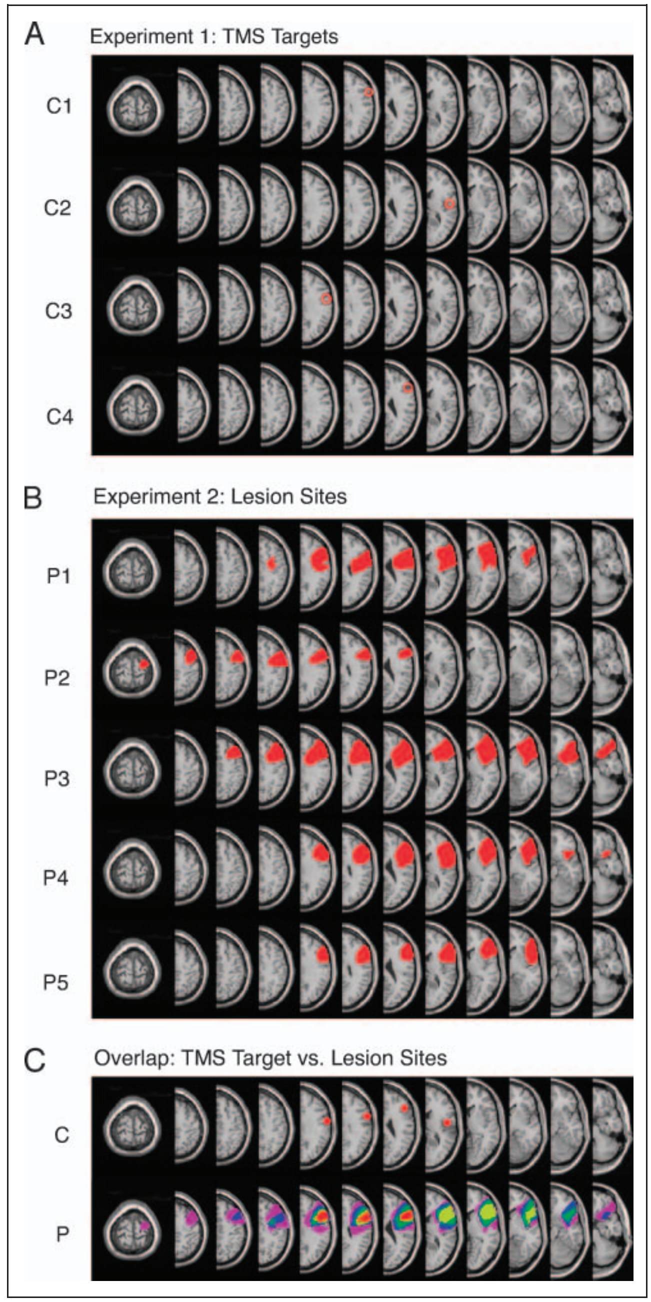

Figure 1. (A) Location of the center of the target sphere for TMS localization for each control participant in Experiment 1. The Montreal Neurological Institute coordinates of the TMS target for each subject were C1 [58, 14, 30], C2 [46, 6, 10], C3 [52, −2, 32], and C4 [46, 32, 24]. (B) Stroke lesion location in each patient in Experiment 2. The scans from patients with left-sided lesions (P1, P3, P4) were mirror flipped to permit its comparison with the patients with right-sided lesions (P2, P5) and the right-sided TMS target site in healthy participants. (C) TMS target sites from each healthy participant are presented on one canonical brain, and lesions from each stroke patient were combined to show the location of maximal overlap (in red color).

METHODS

Participants

The participants in Experiment 1 (TMS experiment) were four students from the University of California at Berkeley (ages 21–28 years, $M = 24.5$ years, two women). All participants were right-handed with normal or corrected-to-normal vision, and none reported any history of neurological or psychiatric problems. The participants in Experiment 2 (patient experiment) were five individuals (ages 44–72 years, $M = 56$ years, two women) with lateral PFC lesions due to stroke. Patients 1, 3, and 4 (P1, P3, and P4, respectively) had left frontal lesions, and Patients 2 and 5 (P2 and P5, respectively) had right frontal lesions (see Figure 1). These patients were selected from our patient pool because they had lesions that encompassed the PFC target region in the TMS experiment (see below). P1 and P3 were tested 8 years poststroke, P2 and P4 were tested 3 years poststroke, and P5 was tested 4 years poststroke. Each participant gave informed written consent before being tested and received monetary compensation upon completion of each phase of the study. The following experimental procedure was conducted in compliance with the Committee for the Protection of Human Subjects at the University of California, Berkeley.

Behavioral Task

During performance of the experimental task, participants viewed 16-sec blocks of 20 face or 20 scene stimuli (in random order) presented for 300 msec each with a 500-msec intertrial interval. There were also "baseline" blocks where subjects had to simply fixate on a centrally presented fixation cross. The task consisted of 7 blocks of each category of stimuli as well as 14 blocks (Experiment 1) or 7 blocks (Experiment 2) of the baseline condition. Thus, the task

was designed to be brief to be completed before the effects of TMS dissipated in Experiment 1 as well as to assure that the patients were able to complete the task in Experiment 2. Moreover, to ensure that participants were viewing the stimuli, they were instructed to make a button press with their right or left index finger any time that an image matched the image immediately preceding it. For each stimulus category, there were only eight trials (across seven blocks) in which there was a matching stimulus requiring a response. Given this small number of trials in which behavioral data could be obtained, comparisons in performance between TMS and baseline sessions within participants or between patients and healthy controls could not provide reliable results. However, given the simple nature of the repetition detection, all participants performed near ceiling on the task demonstrating that they were perceptually encoding the stimuli being presented to them adequately to make the simple match decision. In the TMS experiment, different face and scene stimuli were used between sessions to avoid any familiarity effects, repetition suppression, or other cognitive processes of noninterest due to repeated exposure to images.

Experimental Procedure

In Experiment 1, participants were recruited for two separate experimental sessions. In Session 1, participants performed the experimental task during whole-brain fMRI scanning without any TMS intervention. After Session 1, data were analyzed (see statistical methods below) to identify a target ROI in the lateral PFC that was engaged in that participant during both face versus baseline and scene versus baseline contrasts ($p < .001$, uncorrected; see Figure 1). Although this task consistently activated both hemispheres, the right hemisphere was chosen due to a slight bias of activity toward the right PFC that was observed in a previous group analysis using the identical task (unpublished data). After identification of the targeted PFC region, the subject-specific location of coil placement was determined by overlaying these statistical maps onto each individual's high-resolution T1-weighted MRI images in a frameless stereotaxy system (Rogue-Research Inc., Montreal, Canada) designed for TMS localization. This system allows for the identification of a target ROI with 2-mm precision. Before Session 2, the targeted PFC ROI was first localized on the participants scalp using frameless stereotaxy. An electrode-less EEG cap was placed on each participant, and the location on the scalp overlaying the target cortical area was marked with a fiducial marker. This fiducial marker served two purposes: (1) to guide later coil placement during the TMS/fMRI session and (2) to provide a marker within each anatomical image specifying and confirming the particular cortical areas underlying the central hot-spot of the TMS coil. In Experiment 2, the patients with focal lesions were only scanned once during which they performed the experimental task. Each patient's lesion map as well as a composite map of the overlap of the lesions in each patient is provided in Figure 1.

TMS Parameters (Experiment 1)

In Session 2, the order in which TMS was administered relative to the baseline fMRI session differed between participants. In two participants (C1 and C2), anatomical images were acquired, and then they performed the experimental task in the scanner. Next, participants were removed from the scanner and administered 20 min of 1 Hz repetitive TMS (rTMS) over the target ROI. Participants were then immediately scanned and performed the experimental task again. The other two participants (C3 and C4) were first scanned for positioning and magnet shimming. Next, they were removed from the scanner and administered 20 min of 1 Hz rTMS. Immediately after TMS, they were then placed back into the scanner and performed the first session of the behavioral task. After completion of the experimental task, these participants took a 20-min break in the scanner. After the break, they performed the experimental task a second time to complete the experimental session.

MRI Acquisition and Preprocessing (Experiments 1 and 2)

Functional images were acquired from a Varian INOVA 4-T scanner equipped with a transverse electromagnetic send-and-receive radio-frequency head coil. Functional images were collected using a gradient-echo-planar sequence (repetition time [TR] = 2000 msec, echo time [TE] = 28 msec, matrix size = 64 × 64, field of view [FOV] = 22.4 cm) sensitive to BOLD contrast. Each functional volume consisted of 18 3.5 × 3.5 × 5-mm-thick axial slices with a 0.5-mm gap between each slice, providing whole-brain coverage except for portions of the inferior cerebellum and the most superior extent of the parietal lobe. For each scan, 10 sec of gradient and radio-frequency pulses preceded data acquisition to allow steady-state tissue magnetization. Two T1-weighted anatomical scans were also acquired. In the first, anatomical images coplanar with the EPI data were collected using a gradient-echo multislice sequence (TR = 200 msec, TE = 5 msec, FOV = 22.4 cm^2, matrix size = 256 × 256, in-plane resolution = 0.875 × 0.875 mm). These images were used in later analyses to determine individual-specific ROIs as well as to anatomically localize functional activations. In the second, high-resolution anatomical data were acquired with an MP-FLASH 3-D sequence (TR = 9 msec, TE = 5 msec, FOV = 22.4 × 22.4 × 19.8 cm, matrix size = 256 × 256 × 128, resolution = 0.875 × 0.875 × 1.54 mm) to aid in spatial normalization for random effects group analyses (see below).

After acquisition, MRI data were converted to ANALYZE format. Data were corrected for between-slice timing differences using a sinc interpolation method and were interpolated to 1-sec temporal resolution (half of the total

TR) by combining each shot of half k-space with the bilinear interpolation of the two flanking shots. Subsequent preprocessing and statistical analysis were performed using SPM2 software (http://www.fil.ion.ucl.ac.uk) run under Matlab 6.5 (www.mathworks.com). Functional data for the tasks across sessions were realigned to the first volume acquired in that run to correct for motion-related artifacts. For the participants in Experiment 1, the set of functional data that was collected second (either the post-TMS or baseline scan depending on the order) was then coregistered to the first session to place EPI data from both sessions in the same space for analysis. No smoothing was performed on the functional data to maximize the spatial resolution and to prevent artificial spreading of activity across PFC voxels.

Whole-brain Univariate Analysis

A standard univariate analysis was conducted under the assumptions of the general linear model to isolate voxels in extrastriate cortex that were engaged selectively during face or scene processing. Each block of the task was modeled as a 16-sec epoch and convolved with a canonical hemodynamic response function. Block-related effects were estimated using a subject-specific fixed-effects model, and linear contrasts were computed to isolate voxels significantly activated in face versus baseline and scene versus baseline conditions. These univariate contrasts were used to isolate task-relevant voxels in Experiments 1 and 2 in the analyses described below.

Univariate Analysis: Magnitude of Stimulus-evoked Activity within Extrastriate Cortex

To examine the impact of PFC TMS and lesion on the magnitude of stimulus-evoked BOLD activity within extrastriate cortex, the univariate statistical maps were probed to compute the beta-parameter estimates of both face versus baseline and scene versus baseline conditions within an extrastriate ROI comprising the 30 most statistically significant voxels. These calculated beta-parameter estimates were compared across PFC disruption conditions in each experiment (Experiment 1: baseline vs. post-TMS; Experiment 2: lesion vs. nonlesion hemisphere).

Category Selectivity Analyses

To examine the distinctiveness of face and scene representations within extrastriate cortex, we performed two complementary analyses that compared the spatial patterns of activity between face and scene responsive voxels. Both analyses used the same anatomical extrastriate ROIs for each hemisphere. The boundaries of these ROIs were determined anatomically to include the lingual, fusiform, inferior temporal, and parahippocampal gyri.

Spatial Correlations

Measuring the correlation between spatial patterns of activity evoked by the viewing of face or scene stimuli offers a method for determining the relative distinctiveness of spatial patterns of stimulus-evoked activity. Spatial correlations are relatively insensitive to focal differences in the magnitude of activity that could occur in between conditions (TMS vs. baseline) or hemispheres (lesion vs. healthy). The t values derived from the face versus baseline and scene versus baseline contrasts within an ROI comprising the 30 most statistically significant voxels (derived from a face plus scene versus baseline contrast) were used to form a matrix of multiple voxels that were translated to a linear vector for each condition (Aguirre, 2007), and correlations between the two stimulus categories were tested using a nonparametric test (Kendall rank order correlation). The output of this analysis was the magnitude of the spatial correlation of the patterns of activity evoked by face versus scene stimuli (expressed as a Kendall's tau coefficient). To assess significance of the observed values, we created a simulated distribution via bootstrapping by recalculating the correlation between those same top 30 voxels after randomization. Shuffling was performed 1 million times per subject, which resulted in a Gaussian distribution where 95% of the tau values were within the range of −.22 and .22.

Overlap Analysis

A complementary analysis to spatial correlations was performed, which compared the spatial overlap of voxels that were responsive to either scene or face stimuli. A conceptually similar analysis has been implemented previously (Park et al., 2004). In this analysis, we stepped separately through face versus baseline and scene versus baseline contrast maps in fixed 30 voxel increments (regardless of t value) up to 120 voxels, and at each mask size we calculated the percentage of voxels that exhibited spatial overlap between these two contrasts. Examining a range of mask sizes in this analysis allowed us to avoid biases related to arbitrary selection of the anatomical mask size on the basis of statistical thresholds. This type of overlap analysis method is less sensitive to magnitude or extent-related differences across conditions than a method that creates bin sizes on the basis of t values. It is important to note that there are many possible approaches for assessing the degree of spatial overlap of contrast maps within ROIs. The potential confounds of any analysis of this type was discussed by Kung, Peissig, and Tarr (2007). In this study, however, the overlap analysis was not performed to precisely quantify the degree of segregation of category selectivity representations within extrastriate cortex but rather to determine how category selectivity is altered by the loss of putative PFC top–down signals.

In Experiment 1, the spatial correlation and overlap analyses were performed separately for the baseline and TMS conditions only within the right extrastriate cortex, which

was the same hemisphere as TMS stimulation, and comparisons are made between these two conditions. In Experiment 2, the analyses were performed in the ipsilesional and contralesional extrastriate cortex, and comparisons are made across hemispheres. These comparisons were chosen due to the disproportionate impact of unilateral frontal lesions on ipsilesional systems (Barcelo et al., 2000; Knight, Scabini, & Woods, 1989).

RESULTS

Given the small sample size for each experiment, the results are presented in the form of a multisubject case study. In all presentations of the results, individualized subject data were shown to relate individual-by-individual patterns across the comparisons described below.

Experiment 1: TMS versus Baseline in Healthy Participants

Effect of TMS on BOLD Signal within Lateral PFC

Figure 2 presents the effect of TMS on BOLD signal in lateral PFC beneath the coil location. Participants C1, C2, and C3 exhibited the predicted effect of decreased BOLD signal under the coil in lateral PFC after TMS as compared with baseline. Participant C4 exhibited the opposite effect.

Spatial Correlation Analysis

In Figure 3 and Table 1, the results of the spatial correlation analysis from each of the four control participants is presented. In this analysis, we predicted that PFC disruption after TMS would lead to higher spatial correlations (e.g., less distinctiveness and greater spatial similarity) between stimulus-evoked activity to face stimuli and scene stimuli within extrastriate cortex. Participants C1, C2, and C3 who exhibited decreased lateral PFC BOLD signal after rTMS (see Figure 2) exhibited increased spatial correlations between the patterns of face and scene-evoked activity within extrastriate cortex after TMS relative to baseline. In contrast, participant C4 who did not exhibit decreased PFC BOLD signal after TMS exhibited spatial correlations after TMS relative to baseline in the opposite direction. In all four participants, this pattern of results between the TMS and the baseline condition was present in all mask sizes that were analyzed (30–120 voxels, see Table 1).

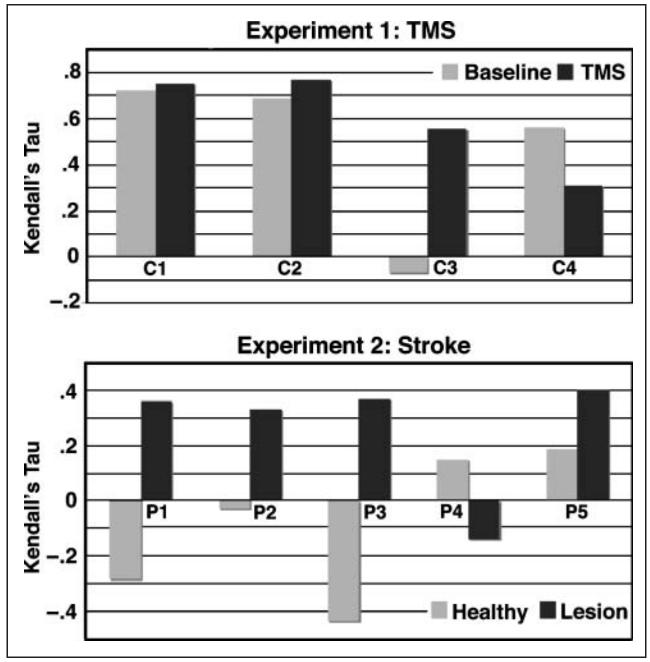

Figure 3. Spatial correlation measures (Kendall's tau coefficient) in face versus baseline and scene versus baseline contrasts following TMS versus baseline in healthy participants (Experiment 1) or within the intact versus lesioned hemisphere in stroke patients (Experiment 2).

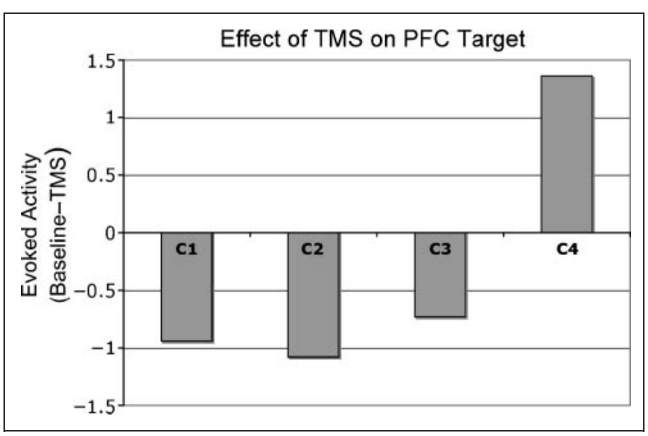

Figure 2. Differences in estimates of PFC BOLD activity beneath the coil after TMS relative to baseline. Parameter estimates reflect the magnitude of task-evoked activity to both categories of stimuli. Negative values reflect greater task-evoked activity during the baseline condition as compared with the TMS condition (suggesting disrupted activity by TMS), whereas positive values reflect greater task-evoked activity after TMS condition as compared with the baseline condition.

Spatial Overlap Analysis

In Table 2, the results of the spatial overlap analysis from each of the four control participants is presented. In this analysis, we predicted that PFC disruption after TMS would lead to increased spatial overlap between voxels responding to face versus scene stimuli within extrastriate cortex. After PFC rTMS, participants C1 and C3 exhibited an increase in the number of voxels within extrastriate cortex that were commonly activated in univariate statistical contrasts of face versus baseline and scene versus baseline conditions. That is, voxels within extrastriate cortex had a higher probability of responding to both stimulus categories rather than showing selectivity to one versus the other. This effect was only present in the smallest mask

Table 1. Spatial Correlation Analysis

	30 Voxels		*60 Voxels*		*90 Voxels*		*120 Voxels*	
	Baseline/Intact	*TMS/Lesion*	*Baseline/Intact*	*TMS/Lesion*	*Baseline/Intact*	*TMS/Lesion*	*Baseline/Intact*	*TMS/Lesion*
C1	.71	.77	.71	.75	.71	.74	.74	.74
C2	.70	.82	.71	.80	.69	.77	.65	.69
C3	−.10	.56	−.11	.57	−.03	.55	−.04	.53
C4	.69	.51	.56	.28	.49	.21	.49	.23
P1	−.51	.37	−.34	.37	−.10	.38	−.10	.31
P2	−.34	.31	−.11	.34	.20	.35	.18	.30
P3	−.59	.22	−.50	.37	−.39	.41	−.26	.45
P4	−.01	−.14	.09	−.17	.22	−.14	.27	−.10
P5	.10	.51	.18	.37	.22	.36	.24	.37

Values represent Kendall's tau coefficients.

size (30 voxels) in participant C2. Participant C4, who did not exhibit decreased PFC BOLD signal after TMS, did not exhibit changes in spatial overlap after TMS relative to baseline in the predicted direction.

Experiment 2: Prefrontal Lesion versus Intact Hemisphere in Stroke Patients

Although TMS can maximally disrupt BOLD signal underneath the central "hot spot" of the coil, there was some evidence suggesting that TMS may exert distal effects on areas functionally connected to the target site (Valero-Cabré, Payne, Rushmore, Lomber, & Pascual-Leone, 2005). As a result, Experiment 2 used another method for investigating the effects of disruption of frontal cortex function—the study of patients with focal lesions due to stroke—to assess the impact of chronic PFC damage on category selectivity in extrastriate cortex. Patients were selected who had lesions in PFC subregions that overlapped with the target site of rTMS in Experiment 1 (see Figure 1) and performed the same behavioral task during fMRI scanning.

Spatial Correlation Analysis

In Figure 3 and Table 1, the results of the spatial correlation analysis from each of the five patient participants is presented. In this analysis, we predicted that a PFC lesion would lead to higher spatial correlations (e.g., less distinctiveness and greater spatial similarity) between stimulus-evoked activity to face stimuli and scene stimuli within extrastriate cortex in the same hemisphere as the lesion as compared with the nonlesioned hemisphere. P1, P2, P3, and

Table 2. Spatial Overlap Analysis

	30 Voxels		*60 Voxels*		*90 Voxels*		*120 Voxels*	
	Baseline/Intact	*TMS/Lesion*	*Baseline/Intact*	*TMS/Lesion*	*Baseline/Intact*	*TMS/Lesion*	*Baseline/Intact*	*TMS/Lesion*
C1	18	21	33	41	54	59	76	81
C2	15	17	38	33	57	54	81	77
C3	5	14	14	27	25	40	34	56
C4	12	10	30	22	49	42	59	60
P1	10	73	28	70	38	68	43	63
P2	27	47	65	63	68	59	75	67
P3	10	67	22	73	33	74	39	73
P4	53	40	63	32	70	41	75	49
P5	20	27	37	47	48	49	51	51

Values represent percentage of voxels that exhibited spatial overlap in the face versus baseline and scene versus baseline contrasts.

P5 exhibited increased spatial correlations in extrastriate cortex within the lesioned hemisphere as compared with the intact hemisphere. P4 did not exhibit the predicted effect. In all four participants, this pattern of results between the lesioned and the intact hemisphere was present in all mask sizes that were analyzed (30–120 voxels, see Table 1).

Spatial Overlap Analysis

In Table 2, the results of the overlap analysis from each of the five patient participants are presented. In this analysis, we predicted that a PFC lesion would lead to increased spatial overlap between voxels responding to face versus scene stimuli within extrastriate cortex in the same hemisphere as the lesion as compared with the nonlesioned hemisphere. P1, P3, and P5 showed an increase in the number of voxels in the extrastriate cortex within the lesioned hemisphere as compared with the intact hemisphere, which was commonly activated in univariate statistical contrasts of face versus baseline and scene versus baseline conditions. P2 and P4 did not exhibit the predicted effects across all mask sizes.

In summary, Experiment 1 demonstrates that after transient disruption of PFC BOLD signal with TMS, activity within extrastriate cortex exhibits decreased category selectivity. This conclusion is bolstered by the observation that the control participant that did not show disruption did not show the effect in the predicted direction. Experiment 2 demonstrates that focal damage to the same PFC sites disrupted by rTMS in Experiment 1 can also lead decreased category selectivity within extrastriate cortex. Unlike Experiment 1, where there is a likely explanation for the one subject that exhibits findings that were not in the predicted direction, there is no obvious explanation for the lack of a predicted effect in P4. P4 did not have a larger lesion or a stroke that occurred at an earlier point in time than the other patients. However, it should be noted that P4 was the only patient to exhibit Kendall tau correlation coefficients from the spatial correlation analysis that were within a range likely to occur by chance (as calculated by a bootstrapping method on shuffled data).

Univariate Analysis: Magnitude of Stimulus-evoked Activity in Extrastriate Cortex

The magnitude of stimulus-evoked activity within extrastriate cortex to both face and scene stimuli is presented in Table 3 for each participant in both experiments. In Experiments 1 and 2, stimulus-evoked activity in extrastriate cortex was greater for faces after TMS relative to baseline in healthy participants and in the lesioned versus intact hemisphere in patients. This pattern of increased stimulus-evoked activity in disruption conditions was less consistent for scene stimuli—it was not observed in one control participant (C2) and two patients (P3 and P4). Interestingly, the two participants that did not exhibit the predicted change in category selectivity in extrastriate cortex (P2 and P4) exhibited different patterns of effects in the magnitude of stimulus-evoked activity. Participant C4, who exhibited the largest increase in stimulus-evoked activity after TMS, and participant P4, who exhibited relatively no difference in stimulus-evoked activity between the lesioned and the intact hemisphere, were the two subjects that did not exhibit the predicted effects regarding changes in category selectivity. These results suggest that increases in the magnitude of stimulus-evoked activity after PFC TMS or after a frontal stroke are not a likely explanation for observed changes in category selectivity. Thus, such changes more likely reflect condition-specific changes (e.g., TMS or lesion) rather than nonspecific factors.

Table 3. Mean Beta-parameter Estimates of the 30 Most Statistically Significant Voxels in Both Face versus Baseline and Scene versus Baseline Contrasts after TMS versus Baseline in Healthy Participants or within the Intact versus Lesioned Hemisphere in Stroke Patients

	Face-Evoked Response		*Scene-Evoked Response*	
	Baseline/Intact	*TMS/Lesion*	*Baseline/Intact*	*TMS/Lesion*
C1	7.4	8.6	7.1	8.3
C2	8.5	8.8	11.4	10.1
C3	8.3	10.3	6.3	9.9
C4	7.0	11.0	7.7	11.0
P1	1.8	3.7	1.9	2.2
P2	3.1	5.2	5.0	7.0
P3	2.0	2.7	3.0	2.7
P4	1.5	1.6	2.2	2.2
P5	1.7	2.4	1.8	3.2

DISCUSSION

Together, the findings from these experiments provide causal evidence for effect of PFC function on the tuning of category representations within human extrastriate cortex. By comparing patterns of brain activity using fMRI during the performance of the same behavioral task after PFC disruption due to rTMS in healthy participants and stroke in patients, convergent evidence was obtained that both transient and permanent disruption of PFC function can alter category selectivity in extrastriate cortex. This work extends the findings of Fuster et al. (1985) in monkeys to humans and suggests that PFC may sharpen the representations of different object categories in extrastriate cortex by increasing the distinctiveness of their distributed neural representations. Similar to the finding that individual inferotemporal neurons lose stimulus selectivity after PFC cooling in monkeys (Fuster et al., 1985), after acute TMS disruption and a chronic focal lesion of PFC in humans, extrastriate cortical activity exhibited less selective responses to different

stimulus categories. This evidence supports an expanded role of PFC in the top–down control of perception and supports a more dynamic rather than rigid representational architecture in the ventral visual stream.

These experiments complement a small but growing literature detailing the causal impact of PFC-mediated top–down signals on visual perception. A wealth of cognitive neuroscience experiments over the past two decades have provided suggestive evidence that activation patterns in PFC track with modulation of bottom–up perceptual responses that are hypothesized to require biasing feedback from top–down influences (for a review, see Miller & D'Esposito, 2005). This suggestive evidence has provided the foundation for several models of PFC function (Postle, 2006; Courtney, 2004; Curtis & D'Esposito, 2003; Miller & Cohen, 2001), purporting that PFC controls multiple dimensions of sensory processing via direct top–down modulatory signals. A major limitation of these models, however, is that without evidence detailing the causal nature of PFC control signals, a complete picture of how PFC sculpts bottom–up perceptual signals remains underspecified.

Recently, several methodological advances have permitted a more detailed characterization of systems-level cortical interactions. Multivariate statistical analyses of fMRI data have shown systematic coupling between PFC and extrastriate cortex in a range of cognitive operations such as mental imagery (e.g., Mechelli, Price, Friston, & Ishai, 2004), strategic memory encoding (e.g., Gazzaley et al., 2007), and active working memory maintenance (e.g., Gazzaley, Rissman, & D'Esposito, 2004). These findings show that enhancement of bottom–up processing of relevant memoranda is accompanied by increased functional connectivity between PFC and extrastriate cortex. Although this coupling could reflect PFC monitoring of bottom–up signals from posterior cortical regions, regional timing measures in neurophysiology (Bar et al., 2006; Rainer et al., 1998) and hemodynamic (Miller, Deouell, Dam, Knight, & D'Esposito, 2008) signals have shown that frontal cortex activity can precede activity in extrastriate cortex—placing PFC subregions in a unique temporal window to influence the first volleys of visual signals through the ventral stream.

Only a few experiments, however, have directly tested the hypothesis that signals from PFC modulate stimulus-evoked activity in posterior cortical regions. In one ERP study, it was found that in patients with focal PFC lesions, bottom–up responses to targets in the attended hemifield are modulated as early as 100 msec after the onset of the stimulus. On the basis of the behavioral relevance of sensory information, these electrophysiology patterns showed that PFC biases evoked signals in both an excitatory and an inhibitory manner (Knight, Staines, Swick, & Chao, 1999; Yamaguchi & Knight, 1990). Stimulating FEF neurons via microstimulation (Moore & Armstrong, 2003) or TMS (Armstrong & Moore, 2007; Ruff et al., 2006) induces biasing shifts in both baseline (i.e., prestimulus) and stimulus-evoked activity in extrastriate cortex. Our findings show that PFC modulates not only the magnitude of neural activity but also the selectivity of these responses during the engagement of object-based attentional processes. Given the overabundance of objects that bombard the visual system at any given moment, object-based attention must bias this representational architecture in favor of task-relevant stimulus categories (Morishima et al., 2009; Bar, 2003). Recent evidence suggests that object-based attention acts via tuning mechanisms that sharpen the representation of relevant objects and suppresses irrelevant objects through a biased competition mechanism (Beck & Kastner, 2009; Desimone, 1998). Although the current task did not introduce competition between simultaneously presented stimulus categories, our evidence suggests that even in a task with minimal attentional demands, feedback from PFC helps to sharpen the boundaries between the representations of different visual object categories. It has also been demonstrated that behavioral performance on working memory tasks can be improved through visual expertise that leads to increased tuning of extrastriate object representations (Moore, Cohen, & Ranganath, 2006).

Several lines of evidence report object-selective visual responses in PFC neurons (Scalaidhe, Wilson, & Goldman-Rakic, 1999; O'Scalaidhe, Wilson, & Goldman-Rakic, 1997) and have shown that the representational codes maintained during task performance in PFC can be dynamically altered on the basis of changes in task instructions and behavioral context (Wallis & Miller, 2003). Some evidence suggests that PFC may maintain codes for particular stimuli of interest that serve as an "attentional template" to bias posterior processing in favor of target stimuli during memory guided attention (Summerfield, Lepsien, Gitelman, Mesulam, & Nobre, 2006). Our findings suggest that PFC may maintain a code for the currently relevant category (e.g., face vs. scene) that could serve to tune the VAC to respond efficiently and sharply to the currently relevant stimulus category. To this end, PFC has been shown to exhibit sensitivity to category boundaries (DeGutis & D'Esposito, 2007; Freedman, Riesenhuber, Poggio, & Miller, 2003), and these PFC responses are rapidly learned in the context of novel categories and also flexibly adjusted on the basis of which category is relevant for behavior (DeGutis & D'Esposito, 2009; Meyers, Freedman, Kreiman, Miller, & Poggio, 2008). Activation of these PFC codes could serve to bias posterior assemblies via direct anatomical connections with the extrastriate cortex or through indirect corticothalamic modulations (Skinner & Yingling, 1976).

In addition to providing evidence for a role of PFC in modulating category selectivity in both the healthy young brain and the damaged brain, these results suggest that PFC signals are the potential source of the decreases in category selectivity in extrastriate cortex that have been observed in normal aging (Park et al., 2004). Given the complex etiology of the aging process, numerous factors could contribute to a decline in the representational specificity of posterior visual association cortex. For example, decreased category selectivity during the aging process has been attributed to a dedifferentiation of cortical responses to sensory

input (Park et al., 2004). Within this model, neural circuits normally tuned to represent specialized visual objects (or, more specifically, particular attributes of those visual objects) lose this selectivity over time and as a result exhibit more generalized response patterns (Li, Lindenberger, & Sikstrom, 2001). Within the visual system, dedifferentiation with aging occurs not just in extrastriate cortex but also within primary visual cortex. Although V1 neurons usually exhibit high selectivity to particular orientations, aging macaques show decreased orientation selectivity and an overall generalized response to multiple orientations (Schmolesky, Wang, Pu, & Leventhal, 2000). Although dedifferentiation is evident at several levels of visual processing (and even possibly at higher heteromodal association regions; for a review, see Rajah & D'Esposito, 2005), a critical gap remains in our understanding of the particular mechanisms driving these findings. Because normal aging experiments require between group comparisons (e.g., aged vs. young controls), they are not optimally suited to tease apart which of a number of covarying structural or physiological changes are at the root of age-related changes in cortical selectivity. Given that we observed strikingly similar changes in category selectivity in extrastriate cortex of healthy controls after TMS to PFC suggests that age-related changes may be due to disruption of top–down PFC signals rather than dedifferentiation of extrastriate cortex. Supporting this possibility that dedifferentiation is driven by nonlocal changes, anatomical studies have not revealed age-related changes in morphology or neural density in the visual cortex with aging (Peters, Nigro, & McNally, 1997; Peters, Feldman, & Vaughan, 1983). This structural data are accompanied by functional evidence reporting preserved fusiform face area activity in normal aging relative to young controls (Grady et al., 1994).

In summary, our preliminary findings demonstrate that PFC plays a causal role in tuning the degree which posterior assemblies in extrastriate cortex exhibit selective responses to discrete object categories. With two different approaches, we report converging evidence that disrupting the fidelity of feedback signals from PFC can lead to decreased distinctiveness in extrastriate cortex to face and scene stimuli. Although the precise mechanism by which PFC mediates these effects requires further research, these experiments highlight a role of PFC in object-based attention and suggest that it may aid behavior by sharpening our distinctions between discrete classes of visual objects.

Acknowledgments

This work was supported by the U.S. National Institutes of Health (grant nos. MH63901 and NS40813) and the Veterans Administration Research Service. The authors are grateful to R. T. Knight and D. Scabini for their help with patient assessment and recruitment and Josh Hoffman for technical assistance.

Reprint requests should be sent to Mark D'Esposito, Helen Wills Neuroscience Institute and Department of Psychology, 132 Barker Hall University of California, Berkeley 94720-3190, or via e-mail: despo@berkeley.edu.

REFERENCES

Aguirre, G. K. (2007). Continuous carry-over designs for fMRI. *Neuroimage, 35,* 1480–1494.

Armstrong, K. M., & Moore, T. (2007). Rapid enhancement of visual cortical response discriminability by microstimulation of the frontal eye field. *Proceedings of the National Academy of Sciences, U.S.A., 104,* 9499–9504.

Bar, M. (2003). A cortical mechanism for triggering top–down facilitation in visual object recognition. *Journal of Cognitive Neuroscience, 15,* 600–609.

Bar, M., Kassam, K. S., Ghuman, A. S., Boshyan, J., Schmid, A. M., Dale, A. M., et al. (2006). Top–down facilitation of visual recognition. *Proceedings of the National Academy of Sciences, U.S.A., 103,* 449–454.

Barcelo, F., Suwazono, S., & Knight, R. T. (2000). Prefrontal modulation of visual processing in humans. *Nature Neuroscience, 3,* 399–403.

Beck, D. M., & Kastner, S. (2009). Top–down and bottom–up mechanisms in biasing competition in the human brain. *Vision Research, 49,* 1154–1165.

Chawla, D., Rees, G., & Friston, K. J. (1999). The physiological basis of attentional modulation in extrastriate visual areas. *Nature Neuroscience, 2,* 671–676.

Courtney, S. M. (2004). Attention and cognitive control as emergent properties of information representation in working memory. *Cognitive, Affective & Behavioral Neuroscience, 4,* 501–516.

Curtis, C. E., & D'Esposito, M. (2003). Persistent activity in the prefrontal cortex during working memory. *Trends in Cognitive Sciences, 7,* 415–423.

DeGutis, J., & D'Esposito, M. (2007). Distinct mechanisms in visual category learning. *Cognitive, Affective & Behavioral Neuroscience, 7,* 251–259.

DeGutis, J., & D'Esposito, M. (2009). Network changes in the transition from initial learning to well-practiced visual categorization. *Frontiers in Human Neuroscience, 3,* 44.

Desimone, R. (1998). Visual attention mediated by biased competition in extrastriate visual cortex. *Philosophical Transactions of the Royal Society of London, Series B, Biological Sciences, 353,* 1245–1255.

Druzgal, T. J., & D'Esposito, M. (2003). Dissecting contributions of prefrontal cortex and fusiform face area to face working memory. *Journal of Cognitive Neuroscience, 15,* 771–784.

Freedman, D. J., Riesenhuber, M., Poggio, T., & Miller, E. K. (2003). A comparison of primate prefrontal and inferior temporal cortices during visual categorization. *Journal of Neuroscience, 23,* 5235–5246.

Fuster, J. M., Bauer, R. H., & Jervey, J. P. (1985). Functional interactions between inferotemporal and prefrontal cortex in a cognitive task. *Brain Research, 330,* 299–307.

Gazzaley, A., Clapp, W., Kelley, J., McEvoy, K., Knight, R. T., & D'Esposito, M. (2008). Age-related top–down suppression deficit in the early stages of cortical visual memory processing. *Proceedings of the National Academy of Sciences, U.S.A., 105,* 13122–13126.

Gazzaley, A., Rissman, J., Cooney, J., Rutman, A., Seibert, T., Clapp, W., et al. (2007). Functional interactions between prefrontal and visual association cortex contribute to top–down modulation of visual processing. *Cerebral Cortex, 17,* 125–135.

Gazzaley, A., Rissman, J., & D'Esposito, M. (2004). Functional connectivity during working memory maintenance. *Cognitive, Affective & Behavioral Neuroscience, 4,* 580–599.

Grady, C. L., Maisog, J. M., Horwitz, B., Ungerleider, L. G., Mentis, M. J., Salerno, J. A., et al. (1994). Age-related changes in cortical blood flow activation during visual

processing of faces and location. *Journal of Neuroscience, 14,* 1450–1462.
Haenny, P. E., & Schiller, P. H. (1988). State dependent activity in monkey visual cortex. I. Single cell activity in V1 and V4 on visual tasks. *Experimental Brain Research, 69,* 225–244.
Haxby, J. V., Gobbini, M. I., Furey, M. L., Ishai, A., Schouten, J. L., & Pietrini, P. (2001). Distributed and overlapping representations of faces and objects in ventral temporal cortex. *Science, 293,* 2425–2430.
Knight, R. T., Scabini, D., & Woods, D. L. (1989). Prefrontal cortex gating of auditory transmission in humans. *Brain Research, 504,* 338–342.
Knight, R. T., Staines, W. R., Swick, D., & Chao, L. L. (1999). Prefrontal cortex regulates inhibition and excitation in distributed neural networks. *Acta Psychologica, 101,* 159–178.
Kung, C. C., Peissig, J. J., & Tarr, M. J. (2007). Is region-of-interest overlap comparison a reliable measure of category specificity? *Journal of Cognitive Neuroscience, 19,* 2019–2034.
Li, S. C., Lindenberger, U., & Sikstrom, S. (2001). Aging cognition: From neuromodulation to representation. *Trends in Cognitive Sciences, 5,* 479–486.
Luck, S. J., Chelazzi, L., Hillyard, S. A., & Desimone, R. (1997). Neural mechanisms of spatial selective attention in areas V1, V2, and V4 of macaque visual cortex. *Journal of Neurophysiology, 77,* 24–42.
Mechelli, A., Price, C. J., Friston, K. J., & Ishai, A. (2004). Where bottom–up meets top–down: Neuronal interactions during perception and imagery. *Cerebral Cortex, 14,* 1256–1265.
Meyers, E. M., Freedman, D. J., Kreiman, G., Miller, E. K., & Poggio, T. (2008). Dynamic population coding of category information in inferior temporal and prefrontal cortex. *Journal of Neurophysiology, 100,* 1407–1419.
Miller, B. T., Deouell, L. Y., Dam, C., Knight, R. T., & D'Esposito, M. (2008). Spatio-temporal dynamics of neural mechanisms underlying component operations in working memory. *Brain Research, 1206,* 61–75.
Miller, B. T., & D'Esposito, M. (2005). Searching for "the top" in top–down control. *Neuron, 48,* 535–538.
Miller, E. K., & Cohen, J. D. (2001). An integrative theory of prefrontal cortex function. *Annual Review of Neuroscience, 24,* 167–202.
Moore, C. D., Cohen, M. X., & Ranganath, C. (2006). Neural mechanisms of expert skills in visual working memory. *Journal of Neuroscience, 26,* 11187–11196.
Moore, T., & Armstrong, K. M. (2003). Selective gating of visual signals by microstimulation of frontal cortex. *Nature, 421,* 370–373.
Morishima, Y., Akaishi, R., Yamada, Y., Okuda, J., Toma, K., & Sakai, K. (2009). Task-specific signal transmission from prefrontal cortex in visual selective attention. *Nature Neuroscience, 12,* 85–91.
Murray, S. O., & Wojciulik, E. (2004). Attention increases neural selectivity in the human lateral occipital complex. *Nature Neuroscience, 7,* 70–74.
Op de Beeck, H. P., Haushofer, J., & Kanwisher, N. G. (2008). Interpreting fMRI data: Maps, modules and dimensions. *Nature Reviews Neuroscience, 9,* 123–135.
O'Scalaidhe, S. P., Wilson, F. A., & Goldman-Rakic, P. S. (1997). Areal segregation of face-processing neurons in prefrontal cortex. *Science, 278,* 1135–1138.
Park, D. C., Polk, T. A., Park, R., Minear, M., Savage, A., & Smith, M. R. (2004). Aging reduces neural specialization in ventral visual cortex. *Proceedings of the National Academy of Sciences, U.S.A., 101,* 13091–13095.
Peters, A., Feldman, M. L., & Vaughan, D. W. (1983). The effect of aging on the neuronal population within area 17 of adult rat cerebral cortex. *Neurobiology of Aging, 4,* 273–282.
Peters, A., Nigro, N. J., & McNally, K. J. (1997). A further evaluation of the effect of age on striate cortex of the rhesus monkey. *Neurobiology of Aging, 18,* 29–36.
Postle, B. R. (2006). Working memory as an emergent property of the mind and brain. *Neuroscience, 139,* 23–38.
Rainer, G., Asaad, W. F., & Miller, E. K. (1998). Memory fields of neurons in the primate prefrontal cortex. *Proceedings of the National Academy of Sciences, U.S.A., 95,* 15008–15013.
Rajah, M. N., & D'Esposito, M. (2005). Region-specific changes in prefrontal function with age: A review of PET and fMRI studies on working and episodic memory. *Brain, 128,* 1964–1983.
Ruff, C. C., Blankenburg, F., Bjoertomt, O., Bestmann, S., Freeman, E., Haynes, J. D., et al. (2006). Concurrent TMS-fMRI and psychophysics reveal frontal influences on human retinotopic visual cortex. *Current Biology, 16,* 1479–1488.
Scalaidhe, S. P., Wilson, F. A., & Goldman-Rakic, P. S. (1999). Face-selective neurons during passive viewing and working memory performance of rhesus monkeys: Evidence for intrinsic specialization of neuronal coding. *Cerebral Cortex, 9,* 459–475.
Schmolesky, M. T., Wang, Y., Pu, M., & Leventhal, A. G. (2000). Degradation of stimulus selectivity of visual cortical cells in senescent rhesus monkeys. *Nature Neuroscience, 3,* 384–390.
Serences, J. T., Saproo, S., Scolari, M., Ho, T., & Muftuler, L. T. (2009). Estimating the influence of attention on population codes in human visual cortex using voxel-based tuning functions. *Neuroimage, 44,* 223–231.
Skinner, J. E., & Yingling, C. D. (1976). Regulation of slow potential shifts in nucleus reticularis thalami by the mesencephalic reticular formation and the frontal granular cortex. *Electroencephalography and Clinical Neurophysiology, 40,* 288–296.
Summerfield, J. J., Lepsien, J., Gitelman, D. R., Mesulam, M. M., & Nobre, A. C. (2006). Orienting attention based on long-term memory experience. *Neuron, 49,* 905–916.
Valero-Cabré, A., Payne, B. R., Rushmore, J., Lomber, S. G., & Pascual-Leone, A. (2005). Impact of repetitive transcranial magnetic stimulation of the parietal cortex on metabolic brain activity: A 14C-2DG tracing study in the cat. *Experimental Brain Research, 163,* 1–12.
Wallis, J. D., & Miller, E. K. (2003). From rule to response: Neuronal processes in the premotor and prefrontal cortex. *Journal of Neurophysiology, 90,* 1790–1806.
Webster, M. J., Bachevalier, J., & Ungerleider, L. G. (1994). Connections of inferior temporal areas TEO and TE with parietal and frontal cortex in macaque monkeys. *Cerebral Cortex, 4,* 470–483.
Womelsdorf, T., Schoffelen, J. M., Oostenveld, R., Singer, W., Desimone, R., Engel, A. K., et al. (2007). Modulation of neuronal interactions through neuronal synchronization. *Science, 316,* 1609–1612.
Yamaguchi, S., & Knight, R. T. (1990). Gating of somatosensory inputs by human prefrontal cortex. *Brain Research, 521,* 281–288.